Mapping Flowfields with a Heated Wire and an Infrared Imaging System

Ehud Gartenberg* and A. Sidney Roberts Jr.†
Old Dominion University, Norfolk, Virginia 23529

Introduction

PLACING a long, electrically heated wire across airflows (wakes, jets, etc.) and measuring its longitudinal temperature variation with an infrared (IR) imaging system can provide information indicative of the air velocity distribution. Local air velocities can be deduced from the wire temperatures through Nusselt number correlations by accounting for, or minimizing and neglecting, the conduction and radiation effects on the wire under steady-state conditions.

Instrumentation

The series of experiments to be addressed centered around an IR imaging system having a single indium-antimonide (InSb) detector, sensitive to IR radiation in the 3.5- to 5.6-μ shortwave band. The lens field of view (FOV) is 20 deg, and the instantaneous field of view (IFOV or pixel) of the detector is 0.0035 rad. The thermograms could be digitized, stored, and analyzed on a personal computer.

Throughout the experiments and the calibration, the target was a 0.076-mm- (0.003-in.-) diam chromel wire placed 0.5 m in front of the IR camera. This wire was part of a chromel-constantan thermocouple assembly that supplied useful temperature readings by itself and also played a key role in the wire emittance calibrations. These calibrations were performed by exposing the region of the thermocouple junction to a hot airstream blown by a heat gun and by adjusting the emittance value in the computer program until the chromel side of the junction showed on the thermogram a temperature identical to that indicated by the thermocouple. In this configuration the wire was an unresolved target, its diameter being smaller than the IFOV. Thus, the value of the apparent emittance found through this calibration was different from the actual (true) emittance of the wire, and it could be used only with experimental setups having identical wire-to-camera distances. With the exception of the wind-tunnel applications, a large cardboard sheet was placed behind the wire to ensure uniformity of the background and to minimize noise associated with it.

Experiments

A feasibility study of the method was performed targeting the wake shed by a cylinder in crossflow, as shown in Fig. 1. A 10-cm-diam cylinder was placed vertically at the beginning of the test section of a 0.9- × 1.2-m low-speed wind tunnel. The electrically heated wire was placed horizontally downstream in the cylinder wake, and the IR camera scanned it from 0.5 m away. A typical result is shown in Fig. 2, where the drop in the temperature of that segment of the wire exposed to the wake is caused by the turbulence-enhanced heat transfer. An extension of this method can use a planar array of heated wires placed across the flowfield of interest to get a two-dimensional picture of the flow. Such an arrangement would make a better use of the two-dimensional scanning capability of the IR camera.

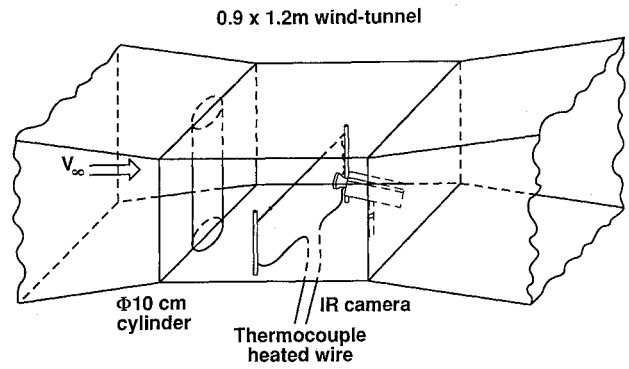

Fig. 1 Experimental layout for IR measurements of a heated wire in the wake of a cylinder.

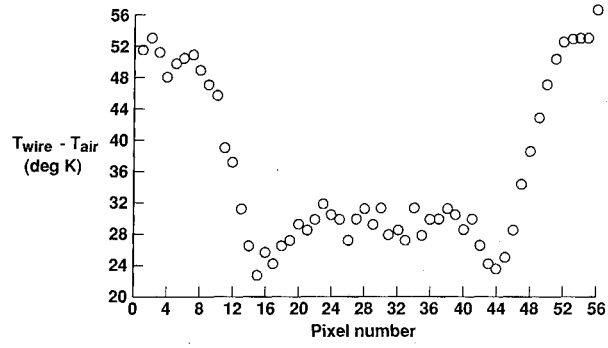

Fig. 2 The wake of a 10-cm-diam cylinder as captured on a heated wire placed 5 cylinder diameters downstream. Re_d = 90,000; 1 pixel = 1.154 mm.

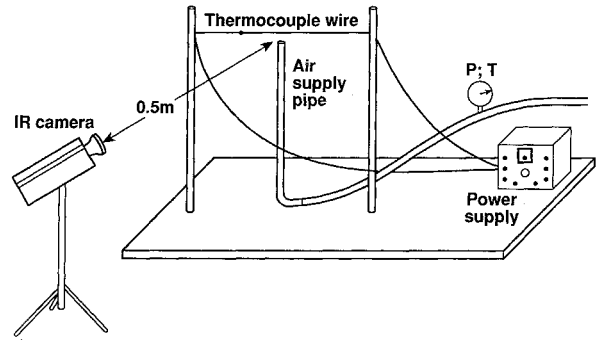

Fig. 3 Setup for the pipe laminar flow heated-wire experiment.

Although this experiment did prove the concept, the structure of the wake flow made it difficult to evaluate the method. Thus, it was decided to abandon this course in favor of the laminar flow at the exit of a round pipe, which, being a simple and ordered flow, offered the opportunity to assess the method in a more convenient way.

As shown in Fig. 3, the electrically heated wire was placed diametrically across the copper pipe 2 mm from its exit. The nominal mean air velocity in the pipe was 2 m/s, and the corresponding Reynolds number based on the pipe diameter was 1700, considered to be within the limit for stable laminar flow.[1] It should be realized that the experiment design faced conflicting requirements: to produce a flow velocity high enough to be measurable with some degree of confidence and at the same time to keep it below the critical Reynolds numbers of transition to turbulence.

The copper pipe had a 13.3-mm i.d., a 15.9-mm o.d., and a length of 102 cm. It was connected to the air outlet through a 5-m-long polyvinyl plastic tube of 15.9-mm i.d. Fine-mesh screens were placed in the pipe 80 cm from its exit to break down vortices or nonuniformities in the flow. This setup was

Received Feb. 10, 1990; revision received June 15, 1990; accepted for publication July 11, 1990.

*Research Assistant Professor, Department of Mechanical Engineering and Mechanics. Senior Member AIAA.

†Professor, Department of Mechanical Engineering and Mechanics.

considered sufficient to provide fully developed laminar flow inside the pipe.[1] The air was supplied by a standard workshop low-pressure system. The air mass-flow rate was monitored by taking pressure and temperature measurements upstream from a sonic nozzle. This pressure was adjusted using a pressure regulator, accounting for the nozzle discharge coefficient and variations in the air temperature, until a nominal centerline velocity of 4 m/s was determined by pitot-tube measurements.

The flow inside the pipe is expected to exhibit the laminar parabolic profile velocity distribution given by

$$U(r) = U_{\max}[1 - (r/R)^2] \qquad (1)$$

where $U(r)$ is the velocity at a distance r from the pipe centerline, $U_{\max}$ is the centerline velocity, and R is the inner radius of the pipe. Good agreement was found between the actual and the parabolic velocity distributions, using a static-pitot tube connected to a water-filled glass manometer inclined 85.5 deg from the vertical. Since the heated wire was placed at the exit of the pipe, the core velocity profile was expected to be very much like the theoretical profile, because the axial velocity of the jet discharging into quiescent atmosphere drops as $1/x$, where x is the axial distance from the jet origin. Observing the heated wire from the pipe centerline outward, three distinct flow regions are encountered: the core flow out of the pipe, the entrainment flow just outside the pipe, and the free convection flow farther on. The following discussion is limited to the segment of the wire that is directly exposed to the pipe core flow.

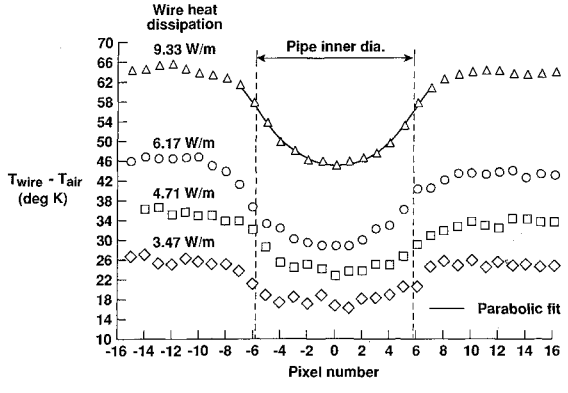

Fig. 4 Heated-wire temperature distribution when exposed to the pipe laminar flow; 1 pixel = 1.154 mm.

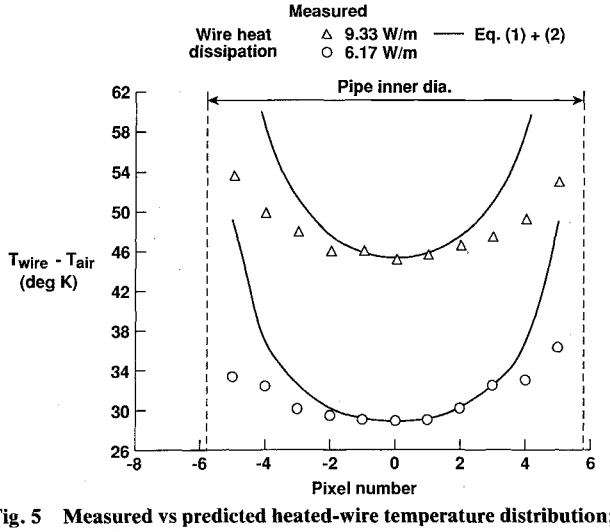

Fig. 5 Measured vs predicted heated-wire temperature distribution; 1 pixel = 1.154 mm.

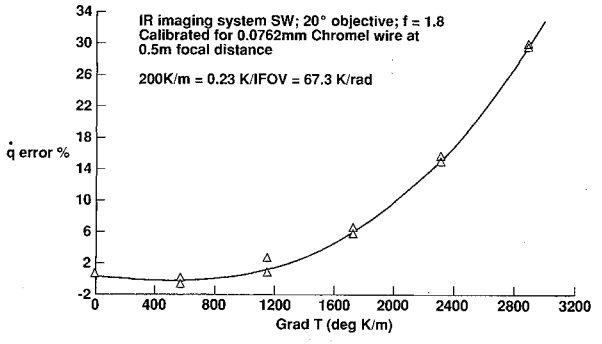

Fig. 6 Error in the thermodynamic heat balance based on the temperature measurements due to the IR camera limitation to track high-gradient temperature distributions. Data based on the experiment with $\dot{q}$ = 9.33 W/m.

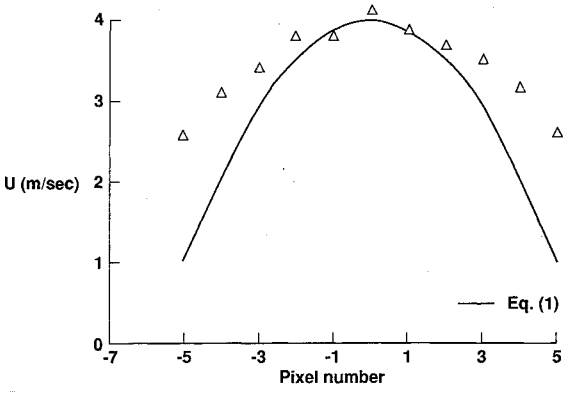

Fig. 7 Velocity profile as deduced from the pipe laminar flow heated-wire measurements ($\dot{q}$ = 9.33 W/m); 1 pixel = 1.154 mm.

The experiments were carried out at four different levels of heating corresponding to dissipation rates of 3.47, 4.71, 6.17, and 9.33 W/m of chromel wire. That part of the wire directly cooled by the core airflow was about one-tenth of the FOV of the IR camera. This design was made purposely to evaluate the system capability to resolve localized temperature changes occurring in the FOV. For each separate experiment nine consecutive frames were taken at a rate of 0.7 Hz, and their average was stored as a single frame for later analysis.

The reduced temperature distributions presented in Fig. 4 show that higher heating levels produce smoother data, probably due to a higher signal-to-noise ratio. At this stage, the accuracy of the measurement was estimated at ± 0.9 K.

To analyze the data, the experimental results were compared with predictions based on a heat transfer correlation,[2] and the parabolic velocity profile [Eq. (1)] given earlier was assumed:

$$Nu_d = 0.795 Re_d^{0.384}, \qquad 1 < Re_d < 35 \qquad (2)$$

where Nu_d and Re_d are the Nusselt and the Reynolds numbers, respectively, both based on the wire diameter d and calculated at discrete distances r from the pipe centerline. The comparison for the two higher heating levels (Fig. 5) shows that the measured temperatures depart systematically from the expected values as measurements proceed along the wire from the centerline outward. The first question was whether correlation (2) is correct or whether the pipe flow was somewhat turbulent, enhancing the heat transfer. These concerns were dropped based on the agreement between the measured and predicted temperatures in the centerline region. Another possibility was that other heat transfer mechanisms may have had a non-negligible influence on the steady-state temperature distribution along the wire. The radiation contribution can be discarded, since it is three orders of magnitude lower than the generated heat. To estimate the conduction contribution, the

measured temperature distribution was approximated by a parabolic fit, from which the temperature gradient was calculated (see the highest heating level data in Fig. 4). Use of the Fourier equation showed the heat-conduction contribution to the cooling of the wire at all stations, except at the centerline (where grad$T$ = 0), to be about two orders of magnitude lower than the generated heat. Thus, the conduction influence can also be discarded.

Another possibility is that measurements with IR imaging systems of targets exhibiting high gradient temperature distributions are consistently lower than what they should be. The extent of this error is unknown (the manufacturer does not supply such information); therefore, an effort was made to estimate it by using the available experimental data. For this purpose, per-pixel calculations were made of

1) the electrical heat dissipation of the wire, based on current and resistance measured values;

2) the heat convected by the air, based on Eqs. (1) and (2);

3) the heat conducted along the wire, based on the measured temperature distribution and the Fourier law of heat conduction; and

4) the heat radiation, based on the measured temperature distribution and the Stephan-Boltzmann law.

Hence, the difference between item 1 and the sum of items 2–4 can be considered as an overall measurement error based on local energy balance. Figure 6 shows this error plotted against the measured temperature gradient at the location of each pixel for the highest heating level experiment. This finding is partially supported by the findings of Boylan et al.,[3] who showed that temperature measurements made with their IR system fell behind the actual temperature distribution once the temperature gradient of the target passed a certain limit (see their Fig. 12).

This conclusion does not diminish the merits of IR imaging systems for aerodynamic research. In fact, if the true error function was known, it would have been possible to adjust the experimental results to get the actual temperature distribution. Starting with the measured distribution, one can iteratively recover the true temperature distribution by adding the measured values distribution and the gradient dependent measurement error. Still to be answered is the question of whether this error is a function of the temperature rate of change of the target in the FOV, or in the IFOV, i.e., to what extent the measurement error is affected by the optics and the distance to the target, in addition to the actual temperature distribution.

In closing, it is suggested that the temperature distribution of the heated wire may be used to reconstruct the flow velocity distribution by using Eq. (2). This application of the method is illustrated in Fig. 7, where the only correction made was to subtract the heat conduction effects along the wire. The implementation of this method has to wait until the actual measurement errors of IR imaging systems are available, and their source understood.

Acknowledgments

This research was partially supported by NASA Langley Research Center Grant NAG1-735.

References

[1]Schlichting, H., *Boundary Layer Theory,* 7th ed., McGraw-Hill, New York, 1979, pp. 39, 241, 242.

[2]Morgan, V. T., "The Overall Convective Heat Transfer from Smooth Circular Cylinders," *Advances in Heat Transfer,* Vol. 11, Pergamon, New York, 1975.

[3]Boylan, D. E., Carver, D. B., Stallings, D. W., and Trimmer, L. L., "Measurement and Mapping of Aerodynamic Heating Using a Remote Infrared Scanning Camera in Continuous Flow Wind Tunnels," *Proceedings of the AIAA 10th Aerodynamic Testing Conference,* AIAA, New York, 1978, pp. 213–231.

Low-Order Panel Method for Internal Flows

K. Sudhakar* and G. R. Shevare†
Indian Institute of Technology, Bombay, India

Introduction

LOW-ORDER panel methods, if properly formulated, can yield accuracy levels comparable to higher order methods even for comparable panel densities.[1,2] Such low-order panel methods are currently popular as design tools in aeronautical industries, especially for external flows. The same ease and confidence is lacking, however, in applying low-order panel methods to internal flows or internal-external flows due to problems of accuracy.[3] A low-order panel method is proposed here that aims at reducing errors in the analysis of internal flows through complex three-dimensional ducts. A synthesized solution technique that can enhance solution accuracy of internal flow analysis or analyze internal-external flows in aircraft-intake combinations is also proposed.

The proposed low-order panel method uses constant source and doublet on flat panel approximations of the geometry to be analyzed. Such a scheme suffers from loss of accuracy as the higher order terms are neglected. This loss of accuracy may in some cases be avoided by using a large number of panels, but only at the cost of increased computations, negating the basic purpose of resorting to a low-order scheme. Since the most significant among the neglected terms in the low-order scheme is the gradient in doublet strength,[4] the accuracy can best be increased if gradients in the doublet distribution are somehow reduced. The proposed formulation aims at providing a handle to reduce gradients in the unknown doublet distribution a priori.

Analysis

The internal flowfield is considered as a perturbation field over an arbitrarily prescribed velocity V_o. The flow problem is solved by a formulation in which the doublet gradients become equal to this perturbation velocity. This is done by prescribing a source distribution of strength $\sigma = (v_n - V_o \cdot n)$ and solving for doublet strength μ by setting the external perturbation potential to zero:

$$\iint_S (v_n - V_o \cdot n)(-1/r)\,\mathrm{d}s + \iint_S \mu \nabla(1/r) \cdot n\,\mathrm{d}s = 0 \Big|_p \tag{1}$$

Here n is the unit normal to the boundary s that points to the internal flow domain, v_n is the desired normal velocity boundary condition, and r is the distance from ds to any point p on the boundary but outside the flow domain. It can be shown that doublet strength μ here is equal to the perturbation potential ϕ on the boundary. The surface velocity along a direction t, therefore, is

$$v_t = (\nabla\phi + V_o) \cdot t = (\nabla\mu + V_o) \cdot t \tag{2}$$

The doublet gradient in this formulation is equal to the surface perturbation velocity and may be reduced by a proper choice

Received May 23, 1990; revision received and accepted for publication July 28, 1990.

*Assistant Professor.
†Professor, Department of Aeronautical Engineering.